

Thermal decomposition of hydrotalcite with chromate, molybdate or sulphate in the interlayer

Ray L. Frost*, Anthony W. Musumeci, Thor Bostrom, J. Theo Kloprogge, Moses O. Adebajo, Matt L. Weier and Wayde Martens

Inorganic Materials Research Program, School of Physical and Chemical Sciences, Queensland University of Technology, GPO Box 2434, Brisbane Queensland 4001, Australia.

Frost, Ray and Musumeci, Anthony and Bostrom, Thor and Martens, Wayde and Adebajo, Moses and Weier, Matt (2005) Thermal decomposition of hydrotalcite with chromate, molybdate or sulphate in the interlayer. *Thermochimica Acta* 429(2):179-187.

Copyright 2005 Elsevier

This is the authors' version of this work.

Abstract:

The thermal decomposition of hydrotalcites with chromate, molybdate and sulphate in the interlayer has been studied using thermogravimetric analysis coupled to a mass spectrometer measuring the gas evolution. X-ray diffraction shows the hydrotalcites have a d(003) spacing of 7.98 Å with very small differences in the d-spacing between the three hydrotalcites. XRD was also used to determine the products of the thermal decomposition. For the sulphate-hydrotalcite decomposition the products were MgO and a spinel MgAl₂O₄, for the chromate interlayered hydrotalcite MgO, Cr₂O₃ and spinel. For the molybdate interlayered hydrotalcite the products were MgO, spinel and MgMoO₄. EDX analyses enabled the formula of the hydrotalcites to be determined. Two processes are observed in the thermal decomposition namely dehydration and dehydroxylation and for the case of the sulphate interlayered hydrotalcite a third process is the loss of sulphate. Both the dehydration and dehydroxylation take place in three steps each for each of the hydrotalcites.

Keywords: hydrotalcite, takovite, pyroaurite, chromate, molybdate, thermal analysis, thermogravimetry

* Author to whom correspondence should be addressed (r.frost@qut.edu.au)

Introduction

Hydrotalcites or layered double hydroxides (LDHs) are fundamentally anionic clays, and are less well-known than cationic clays like smectites. The structure of hydrotalcite can be derived from a brucite structure ($\text{Mg}(\text{OH})_2$) in which e.g. Al^{3+} or Fe^{3+} (pyroaurite-sjögrenite) substitutes a part of the Mg^{2+} . Further mixtures of these mineral phases with multiple anions in the interlayer are observed. When LDHs are synthesized any appropriate anion can be placed in the interlayer. This substitution creates a positive layer charge on the hydroxide layers, which is compensated by interlayer anions or anionic complexes [1, 2]. The hydrotalcite may be considered as a gigantic cation which is counterbalanced by anions in the interlayer. In hydrotalcites a broad range of compositions are possible of the type $[\text{M}^{2+}_{1-x}\text{M}^{3+}_x(\text{OH})_2][\text{A}^{n-}]_{x/n} \cdot y\text{H}_2\text{O}$, where M^{2+} and M^{3+} are the di- and trivalent cations in the octahedral positions within the hydroxide layers with x normally between 0.17 and 0.33. A^{n-} is an exchangeable interlayer anion [3]. In the hydrotalcites reevesite and pyroaurite, the divalent cations are Ni^{2+} and Mg^{2+} respectively with the trivalent cation being Fe^{3+} . In these cases the carbonate anion is the major interlayer counter anion. Of course when synthesizing hydrotalcites any anion may be used. Normally the hydrotalcite structure based upon takovite (Ni,Al) and hydrotalcite (Mg,Al) has basal spacings of $\sim 8.0 \text{ \AA}$ where the interlayer anion is carbonate.

Thermal analysis using thermogravimetric techniques (TG) enables the mass loss steps, the temperature of the mass loss steps and the mechanism for the mass loss to be determined. Thermoanalytical methods provide a measure of the thermal stability of the hydrotalcite.

The reason for the potential application of hydrotalcites as catalysts rests with the ability to make mixed metal oxides at the atomic level, rather than at a particle level. One would expect that the potential application of hydrotalcites as catalysts will rest on reactions occurring on their surfaces. The significance of the formation of the mixed metal oxides is their importance as a transition material in the synthesis of catalysts. In this work we report the thermogravimetric analysis of hydrotalcite with sulphate, chromate or molybdate in the interlayer.

Experimental

Synthesis of hydrotalcite compounds:

A mixed solution of aluminium and magnesium nitrates ($[Al^{3+}] = 0.25M$ and $[Mg^{2+}] = 0.75M$; $1M = 1mol/dm^3$) and a mixed solution of sodium hydroxide ($[OH^-] = 2M$) and the desired anion, at the appropriate concentration, were placed in two separate vessels and purged with nitrogen for 20 minutes (all compounds were dissolved in freshly decarbonated water). The cationic solution was added to the anions via a peristaltic pump at $40mL/min$ and the pH maintained above 9. The mixture was then aged at $75^\circ C$ for 18 hours under a N_2 atmosphere. The resulting precipitate was then filtered thoroughly, with room temperature decarbonated water to remove nitrates and left to dry in a vacuum desiccator for several days. In this way hydrotalcites with different anions in the interlayer were synthesised.

The phase composition was checked by X-ray diffraction and the chemical composition by EDXA analyses.

X-ray diffraction

X-Ray diffraction patterns were collected using a Philips X'pert wide angle X-Ray diffractometer, operating in step scan mode, with $Cu K_\alpha$ radiation (1.54052 \AA). Patterns were collected in the range 3 to $90^\circ 2\theta$ with a step size of 0.02° and a rate of $30s$ per step. Samples were prepared as a finely pressed powder into aluminium sample holders. The Profile Fitting option of the software uses a model that employs twelve intrinsic parameters to describe the profile, the instrumental aberration and wavelength dependent contributions to the profile.

SEM and X-ray microanalysis

Hydrotalcite samples were coated with a thin layer of evaporated carbon and secondary electron images were obtained using an FEI Quanta 200 scanning electron microscope (SEM). For X-ray microanalysis (EDX), three samples were embedded in

Araldite resin and polished with diamond paste on Lamplan 450 polishing cloth using water as a lubricant. The samples were coated with a thin layer of evaporated carbon for conduction and examined in a JEOL 840A analytical SEM at 25kV accelerating voltage. Preliminary analyses of the hydrotalcite samples were carried out on the FEI Quanta SEM using an EDAX microanalyser, and microanalysis of the clusters of fine crystals was carried out using a full standards quantitative procedure on the JEOL 840 SEM using a Moran Scientific microanalysis system. Chromite was used as a standard for Cr, molybdate for Mo, anhydrite for S. Almandine garnet and pyrope garnet were also used in the calibration of the EDX analyses. Oxygen was not measured directly but was calculated using assumed stoichiometries to the other elements analysed.

Thermal Analysis

Thermal decompositions of the hydrotalcites were carried out in a TA® Instruments incorporated high-resolution thermogravimetric analyzer (series Q500) in a flowing nitrogen atmosphere (80 cm³/min). Approximately 50mg of sample was heated in an open platinum crucible at a rate of 2.0 °C/min up to 1000°C. The TGA instrument was coupled to a Balzers (Pfeiffer) mass spectrometer for gas analysis. The following gases were analyzed: CO, CO₂, SO₂, SO₃, and H₂O. Mass/charge ratios are measured for example O₂ is 32/1 and 32/2.

Band component analysis of the DTG curves was undertaken using the Jandel 'Peakfit' software package, which enabled the type of fitting function to be selected and allows specific parameters to be fixed or varied accordingly. Band fitting was done using a Gauss-Lorentz cross-product function with the minimum number of component bands used for the fitting process. The Gauss-Lorentz ratio was maintained at values greater than 0.7 and fitting was undertaken until reproducible results were obtained with squared correlations of r^2 greater than 0.995.

Results and discussion

X-ray diffraction

The X-ray diffraction patterns of the hydrotalcite of formula $(\text{Mg}_6\text{Al}_2(\text{OH})_{16}(\text{XO}_4)_2 \cdot 4\text{H}_2\text{O})$ where X is S, Cr or Mo is shown in **Figure 1**. The figure clearly shows the X-ray pattern for hydrotalcite with no peaks due to other phases. The d(003) spacing for the sulphate, chromate and molybdate interlayered hydrotalcites are 7.99, 7.98 and 7.97 Å respectively. Such values are close to the d-spacing values reported for the natural hydrotalcite with sulphate in the interlayer [4].

The XRD of the products of the thermal decomposition of the chromate interlayered hydrotalcite shows that MgO (JCPD file 45-0946), Cr_2O_3 (01-1294) and spinel (75-1798) are formed (**Figure 2**). The products of the thermal decomposition of the molybdate-hydrotalcite were MgO, MgMoO_4 (21-0961) and MgAl_2O_4 . The products of the sulphate-hydrotalcite were a mixture of the oxides of Mg and Al. These types of products are in agreement with published data [5].

EDX analyses

The EDX analyses are illustrated by Figures 3a, 3b and 3c, being the analyses for the hydrotalcite interlayered with chromate, molybdate and sulphate. The results of nine analyses are reported in **Table 1**. In all three analyses the ratio of Mg to Al is slightly less than the theoretical value of 3:1. For the chromate interlayered hydrotalcite the value is 2.771, for the molybdate interlayered hydrotalcite the value is 2.89 and for the sulphate interlayered hydrotalcite the value is 2.75. The surface of the brucite structure should have no charge per Mg atom. When a trivalent anion is substituted for the Mg such as Al, a charge of 1 is introduced. For two Al atoms the charge is 2. Thus this positive charge will be counterbalanced by the anions chromate, molybdate or sulphate. The ratio of Al to anion is theoretically 2:1. For the chromate interlayered hydrotalcite the ratio of Al:Cr is 6.20, for the molybdate interlayered hydrotalcite the value is 4.70 and for the sulphate interlayered hydrotalcite the value is 5.06. Thus the ratio of the moles of the anions is low compared with the theoretical value. The EDX analyses clearly show no impurities. No C for carbonate or N for

nitrate is present within the limits of the experiment. Thus it is concluded that the balance of the negative charge must be due to hydroxyl ions in the interlayer. Vibrational spectroscopy supports this conclusion as no carbonate or nitrate bands were found in the Raman spectra of the hydrotalcite. Thus the formula of the synthetic hydrotalcites interlayered with chromate may be given by $\text{Mg}_6\text{Al}_2(\text{OH})_{16}(\text{CrO}_4, \text{OH}) \cdot 4\text{H}_2\text{O}$ and similarly for the hydrotalcite interlayered with molybdate and sulphate.

Thermogravimetry and Mass spectrometric analysis of the chromate-hydrotalcite

High resolution thermogravimetry can measure to six decimals of mass enabling subtle mass loss steps to be obtained. This enables changes in stoichiometries to be made. Phase changes would need to be identified using XRD. When the TG is converted to a DTG curve then additional information often differentiating between closely overlapping mass loss steps can be obtained. The use of evolved gas mass spectrometry when coupled to the TG allows definitive identification of the evolved gases. Normally the DTG curve matches the evolved gas mass spectrum curve. Such techniques have been used to study quite complex mineralogical systems [6-10].

The thermogravimetric analysis of hydrotalcite with chromate as in the counterbalancing ion is shown in **Figure 4**. The ion current graphs reporting the mass of evolved gases is shown in **Figure 5**. Five mass loss steps are observed at 99, 192, 354, 427 and 452 °C which correspond to percentage mass losses of 7.4, 4.8, 10.1, 10.4 and 3.8. An additional mass loss of 2.6 % occurs over a temperature range centred on 498 °C. The ion current curves for masses 18, 17 and 16 show that water is evolved at around 109, 191, 349 and 446 °C. This means that water and/or OH units are being lost at these temperatures. The mass loss of 44 (CO_2) proves that some carbonate is present which decomposes to CO_2 at 354 and 414 °C. Evolved oxygen is observed at 463, 490 and 618 °C but appears to be lost continuously over an extended temperature range.

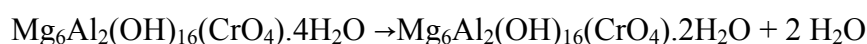
The first two mass loss steps are attributed to the removal of water from the hydrotalcite interlayer. The mass loss steps at 354, 427 and 452 °C are attributed to the dehydroxylation of the chromate interlayered hydrotalcite. The mass loss changes at 498 and the long range temperature decrease in mass is assigned to a loss of oxygen. The theoretical mass loss based upon the formula $\text{Mg}_6\text{Al}_2(\text{OH})_{16}(\text{CrO}_4)\cdot 4\text{H}_2\text{O}$ for the loss of water is 10.9 %, and for the OH units is 21.8 %. The experimental mass loss for water if the first two steps are assumed to be the mass losses due to dehydration, 12.2 %. This value is slightly higher than the theoretical value and may be due to adsorbed water. Therefore the compound may be hydrated with more than four water units in the formula. The DTG profile for temperature range from 240 to 440 °C shows three dehydroxylation steps. The relative areas of the three DTG peaks are 10.2, 10.47 and 4.55 % which is approximately a ratio of 10, 10 to 5. Thus the ratio of moles of OH units lost in these three steps is 2:2:1.

Mechanism for the decomposition of hydrotalcite with chromate in the interlayer

The following steps describe the thermal decomposition of the chromate hydrotalcite.

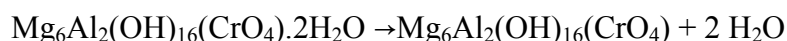
Step 1 at 99 °C

This step includes the loss of adsorbed water.



This step represents the first dehydration step and shows two moles of water are lost at this temperature.

Step 2 at 192 °C



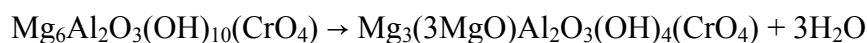
This step represents the second dehydration step and shows two moles of water are lost at this temperature.

Step 3 at 354 °C



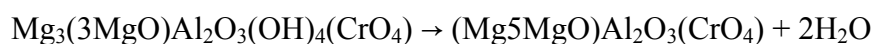
This step represents the first dehydroxylation step and 6 OH units are lost at this temperature. The oxygen is taken up by the cations present and is shown representatively as Al_2O_3

Step 4 at 416 °C



This step represents the second dehydroxylation step and 6 OH units are lost at this temperature.

Step 5 at 452 °C



This step represents the third dehydroxylation step and 4 OH units are lost at this temperature.

Step 6 at 498 °C



This step shows that oxygen is lost and the final products of the thermal decomposition step are the oxides of Cr and Mg and a magnesium aluminate (spinel).

Thermogravimetry and Mass spectrometric analysis of the molybdate-hydrotalcite

The TG and DTG of molybdate-hydrotalcite are shown in [Figure 6](#) and the ion current curves of the evolved gases in [Figure 7](#). The TG analysis shows five mass loss steps at 94, 189, 415, 433 and 481 °C with mass losses of 8.3, 7.0, 12.4, 9.1 and [3.6 %](#). The ion current curves show that water is evolved in each of these steps except the final step. The MS=44 ion current curve shows that some CO_2 is lost indicating the presence of some carbonate in the interlayer as well as the molybdate ion. Raman spectroscopy shows that the amount of carbonate is at very low concentrations. This simply shows the difficulty of keeping CO_2 out of the preparation route for the synthesis of the molybdate-hydrotalcite. The total mass loss of the thermal decomposition is 40.3 %. From the mass of the final products it is calculated that

there were 7 moles of water in the starting material. Thus the molybdate interlayered hydrotalcite is similar to a hydrohonneseite in formulation.

Mechanism for the decomposition of hydrotalcite with molybdate in the interlayer

The following steps describe the thermal decomposition of the molybdate hydrotalcite.

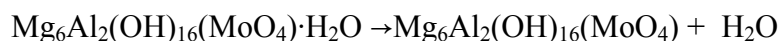
Step 1 at 94 °C

This step includes the loss of adsorbed water.



This step represents the first dehydration step and shows three moles of water are lost at this temperature.

Step 2 at 189 °C



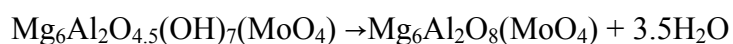
This step represents the second dehydration step and shows one mole of water are lost at this temperature.

Step 3 at 404 °C



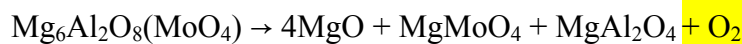
The DTG curve for the 330 to 450 °C may be curve resolved with two peaks at 404 and 433 °C with relative areas of 12.0 and 9.5 %. If these mass loss steps are ascribed to the loss of the OH units then it is suggested that 9 OH units are lost at 404 °C and 7 at 433 °C. This step at 404 °C represents the first dehydroxylation step and 9 OH units are lost at this temperature. The oxygen is taken up by the cations present and is shown representatively as Al₂O₃

Step 4 at 433 °C



This step represents the second dehydroxylation step and 7 OH units are lost at this temperature.

Step 5 at 481 °C



This step shows the final thermal decomposition step.

Thermogravimetry and Mass spectrometric analysis of the sulphate-hydrotalcite

The TG and DTG curves for sulphate-hydrotalcite are shown in [Figure 8](#) and the ion current curves for the gas evolution in [Figure 9](#). Three mass loss steps are observed at 56, 110 and 198 °C which are attributed to dehydration. The total mass loss for these three steps is 13.9 %. The theoretical mass loss based on 4 water units in the structure is 11.12 % which is in agreement with the experimental value. This value is slightly larger as it includes some adsorbed water. Three mass loss steps are observed at 363, 437 and 476 °C with mass loss steps of 5.2, 15.4 and 4.6 %. The first two steps are assigned to dehydroxylation and the last step to a loss of oxygen. The theoretical mass loss for 16 OH units is 22.57 % which is slightly higher than the experimental value of 20.6 %. It is noted some oxygen is lost at 484 °C which would increase the experimental mass loss. A higher mass loss step is observed at 928 °C which is accounted for by the loss of sulphate. The theoretical mass loss of sulphate is 10%. Trace amounts of carbonate in the interlayer may account for this lower than expected value. This would increase the mass loss over the 450 to 500 °C and decrease the mass loss at 928 °C. It is very difficult to synthesise hydrotalcites with no carbonate in the interlayer [11].

Mechanism for the decomposition of hydrotalcite with sulphate in the interlayer

The following steps describe the thermal decomposition of the sulphate interlayered hydrotalcite.

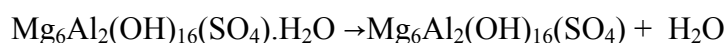
Step 1 at 110 °C

This step includes the loss of adsorbed water.



This step represents the first dehydration step and shows three moles of water are lost at this temperature. The relative areas of the DTG profile at 110 and 198 °C are 10.5 to 3.03 %. This means the loss of water at 110 °C is 3 moles with a further loss of water at 198 °C of one mole.

Step 2 at 198 °C



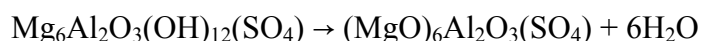
This step represents the second dehydration step and shows one mole of water is lost at this temperature.

Step 3 at 363 °C



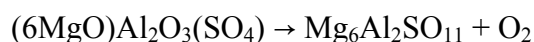
This step represents the first dehydroxylation step and 4 OH units are lost at this temperature. The oxygen is taken up by the cations present and is shown representatively as Al_2O_3 .

Step 4 at 437 °C



This step represents the second dehydroxylation step and 12 OH units are lost at this temperature.

Step 5 at 498 °C



Oxygen is lost at this step.

Step 5 at 928 °C



This step shows that sulphur dioxide is lost and the final products of the thermal decomposition step are the oxide of Mg and a magnesium aluminate (spinel). The upper limit of the TG experiment is 1000 °C and it is possible that some sulphate is retained to a higher temperature. Thus the expected mass loss of 10 % becomes in the experiment 5.2 %.

Conclusions

The thermal decomposition of hydrotalcites based upon a Mg/Al ratio of 3/1 with chromate, sulphate and molybdate in the interlayer has been studied using thermal analysis techniques complimented with X-ray diffraction. The products of the thermal decomposition depend upon the particular interlayer anion. Two processes are observed in the thermal decomposition firstly dehydration and secondly dehydroxylation. Each of these processes takes place in several steps. Mechanisms were proposed for each of the steps in the thermal decomposition.

Acknowledgements

The financial and infra-structure support of the Queensland University of Technology Inorganic Materials Research Program of the School of Physical and Chemical Sciences is gratefully acknowledged. The Australian Research Council (ARC) is thanked for funding the thermal analysis facility.

References

1. R. M. Taylor, *Clay Minerals* 17 (1982) 369.
2. H. F. W. Taylor, *Mineralogical Magazine and Journal of the Mineralogical Society* (1876-1968) 37 (1969) 338.
3. H. C. B. Hansen and C. B. Koch, *Applied Clay Science* 10 (1995) 5.
4. J. T. Kloprogge, D. Wharton, L. Hickey and R. L. Frost, *American Mineralogist* 87 (2002) 623.
5. M. J. Hernandez, M. A. Ulibarri, J. L. Rendon and C. J. Serna, *Thermochimica Acta* 81 (1984) 311.
6. R. L. Frost, Z. Ding and H. D. Ruan, *J. Therm. Anal. Calorim.* 71 (2003) 783.
7. E. Horvath, R. L. Frost, E. Mako, J. Kristof and T. Cseh, *Thermochim. Acta* 404 (2003) 227.
8. E. Horvath, J. Kristof, R. L. Frost, A. Redey, V. Vagvolgyi and T. Cseh, *J. Therm. Anal. Calorim.* 71 (2003) 707.
9. J. T. Kloprogge, J. Kristof and R. L. Frost, 2001 a Clay Odyssey, Proceedings of the International Clay Conference, 12th, Bahia Blanca, Argentina, July 22-28, 2001 (2003) 451.
10. R. L. Frost, E. Horvath, E. Mako, J. Kristof and A. Redey, *Thermochim. Acta* 408 (2003) 103.
11. C. Le Bail, J. H. Thomassin and J. C. Touray, *Physics and Chemistry of Minerals* 14 (1987) 377.

Molybdate							
	Scan 1		Scan 2		Scan 3		Average
Element	Weight %	Mole %	Weight %	Mole %	Weight %	Mole %	Mole %
Mg	22.32	17.64	22.87	18.2	22.58	17.71	17.85
Al	8.62	6.14	8.7	6.24	8.66	6.12	6.17
O	62.32	74.87	61.29	74.13	62.95	75.01	74.67
Mo	6.75	1.35	7.14	1.44	5.81	1.15	1.31
Sulphate							
	Scan 1		Scan 2		Scan 3		Average
Element	Weight %	Mole %	Weight %	Mole %	Weight %	Mole %	Mole %
Mg	24.49	18.68	24.83	18.9	23.33	17.63	18.40
Al	9.79	6.73	10.09	6.92	9.41	6.41	6.69
O	62.99	73.01	63.15	73.06	65.02	74.68	73.58
S	2.72	1.57	1.92	1.11	2.24	1.29	1.32
Chromate							
	Scan 1		Scan 2		Scan 3		Average
Element	Weight %	Mole %	Weight %	Mole %	Weight %	Mole %	Mole %
Mg	23.65	18.01	23.9	18.32	24.98	19.38	18.57
Al	9.38	6.43	9.6	6.63	10.09	7.05	6.70
O	64.58	74.71	63.52	73.98	61.28	72.25	73.65
Cr	2.38	0.85	2.98	1.07	3.65	1.32	1.08

Table 1 EDX analyses of the synthetic hydroxalces interlayered with chromate, molybdate and sulphate

List of Figures

Figure 1 XRD patterns of the hydrotalcite interlayered with sulphate, molybdate or chromate

Figure 2 XRD patterns of the thermal decomposition products of the hydrotalcite interlayered with chromate, molybdate and sulphate together with the patterns of the reference materials.

Figure 3 EDX analyses of the hydrotalcite interlayered with (a) chromate, (b) molybdate and (c) sulphate.

Figure 4 TG and DTG patterns of chromate interlayered hydrotalcite

Figure 5 Thermal evolved gas analysis (ion current curves) of chromate interlayered hydrotalcite for selected gases

Figure 6 TG and DTG patterns of molybdate interlayered hydrotalcite

Figure 7 Thermal evolved gas analysis (ion current curves) of molybdate interlayered hydrotalcite for selected gases

Figure 8 TG and DTG patterns of sulphate interlayered hydrotalcite

Figure 9 Thermal evolved gas analysis (ion current curves) of sulphate interlayered hydrotalcite for selected gases

List of Tables

Table 1 EDX analyses of the synthetic hydrotalcites interlayered with chromate, molybdate and sulphate

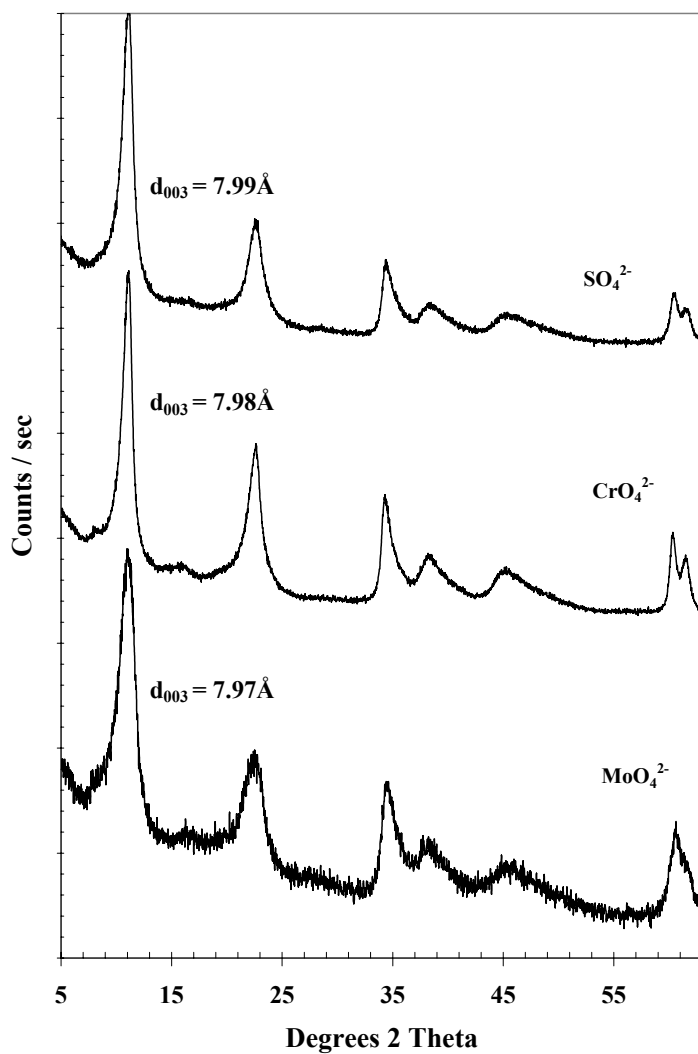


Figure 1 X-ray diffraction patterns of the d(003) spacing of hydrotalcite with different anions in the interlayer.

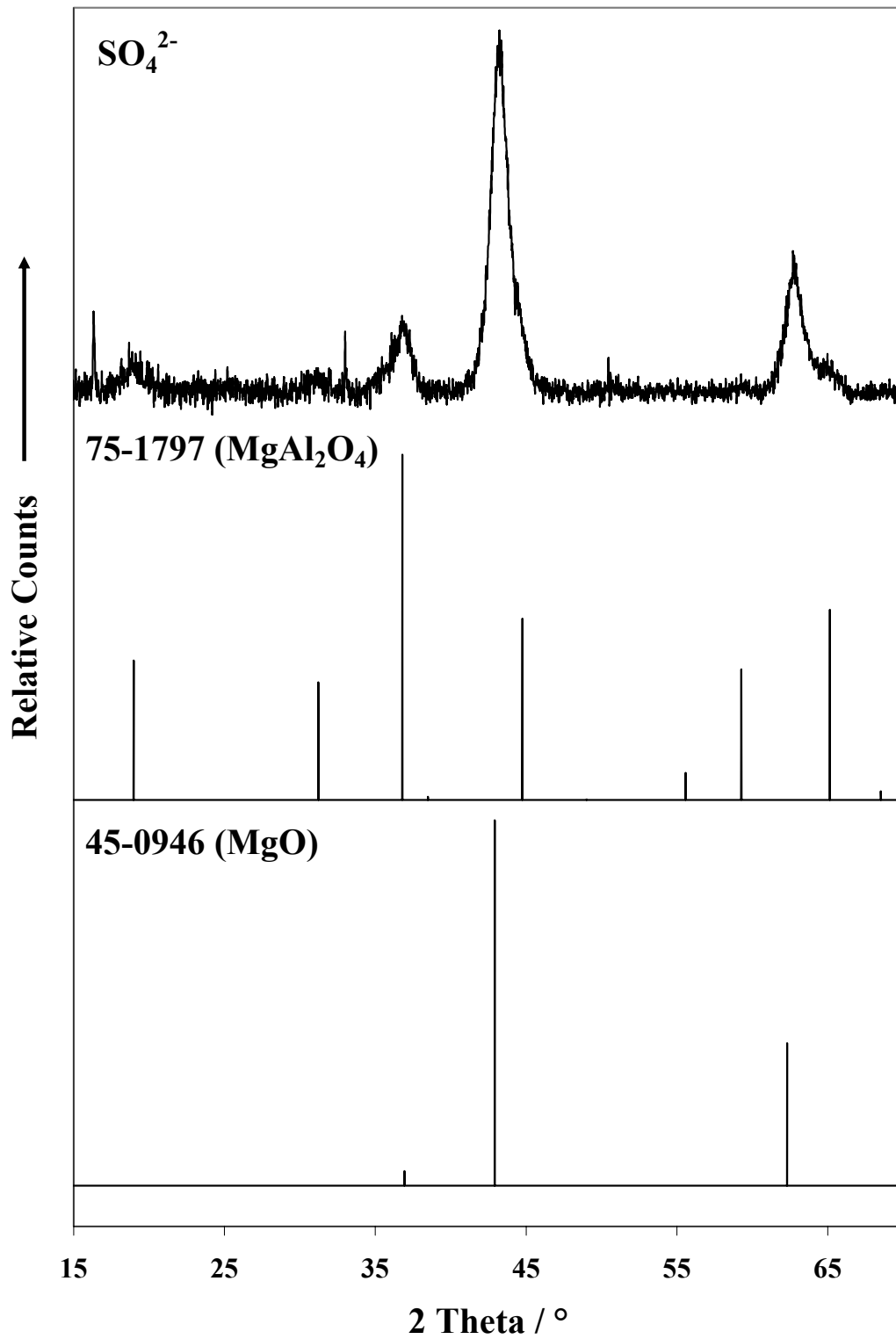


Figure 2c

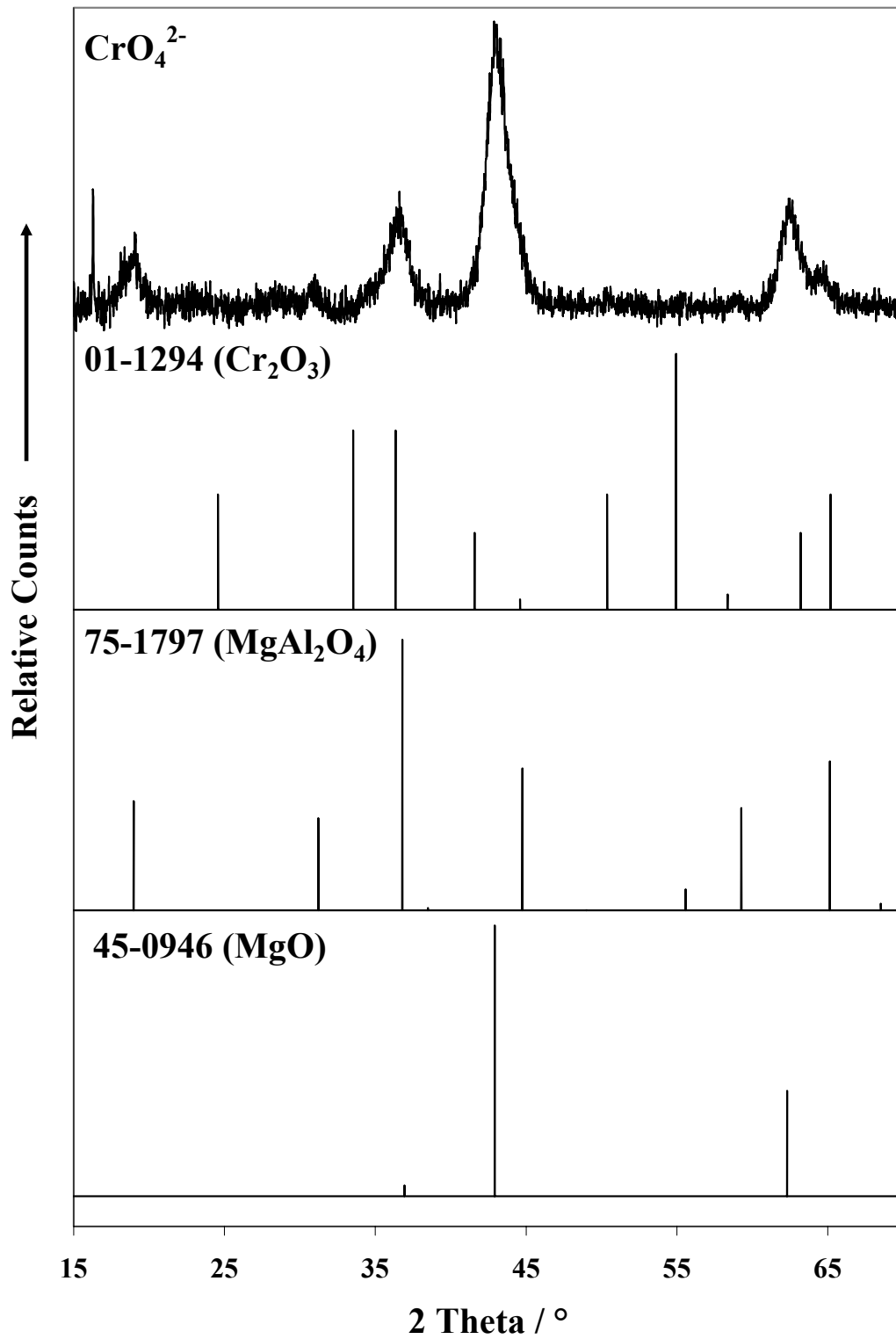


Figure 2b

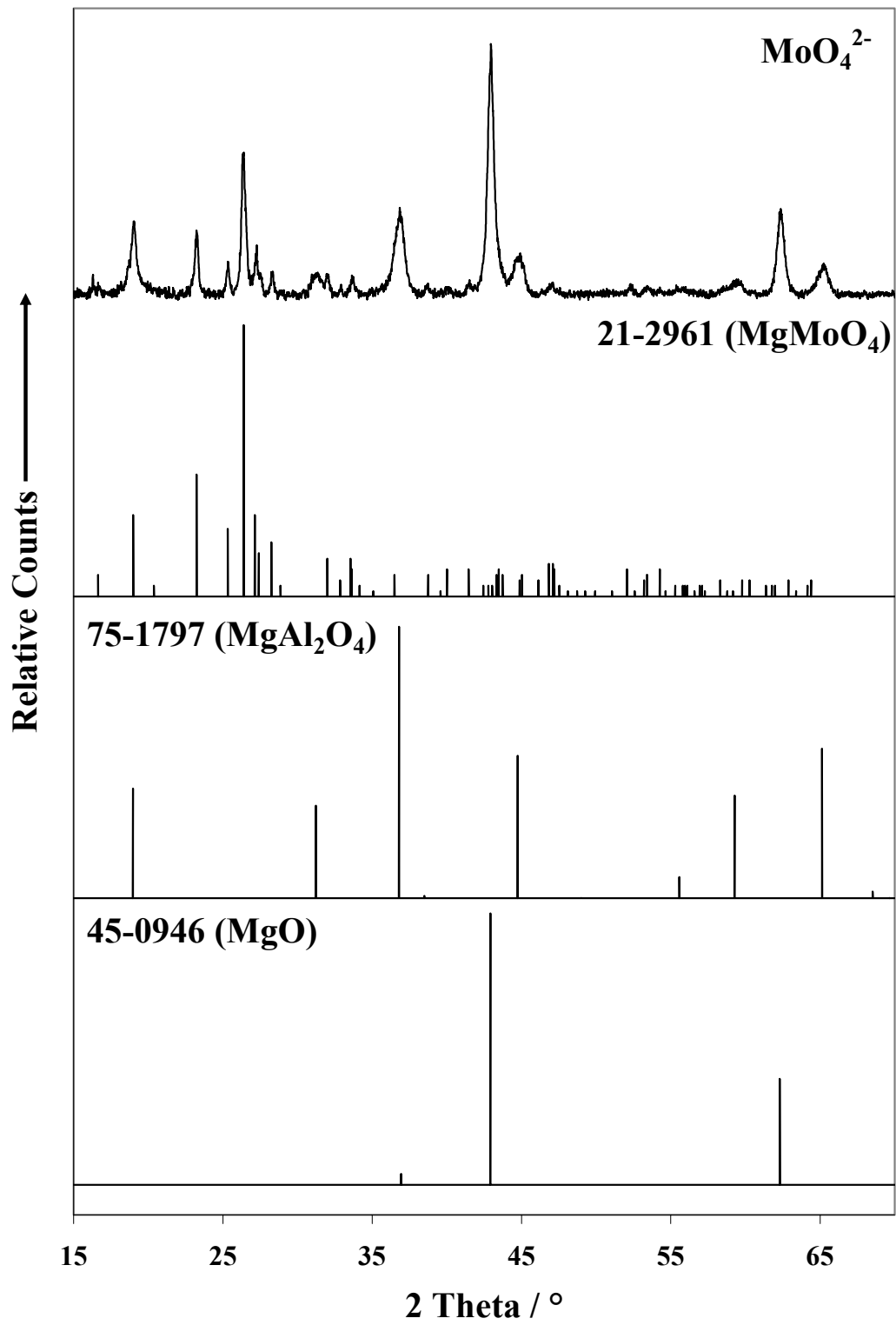


Figure 2a

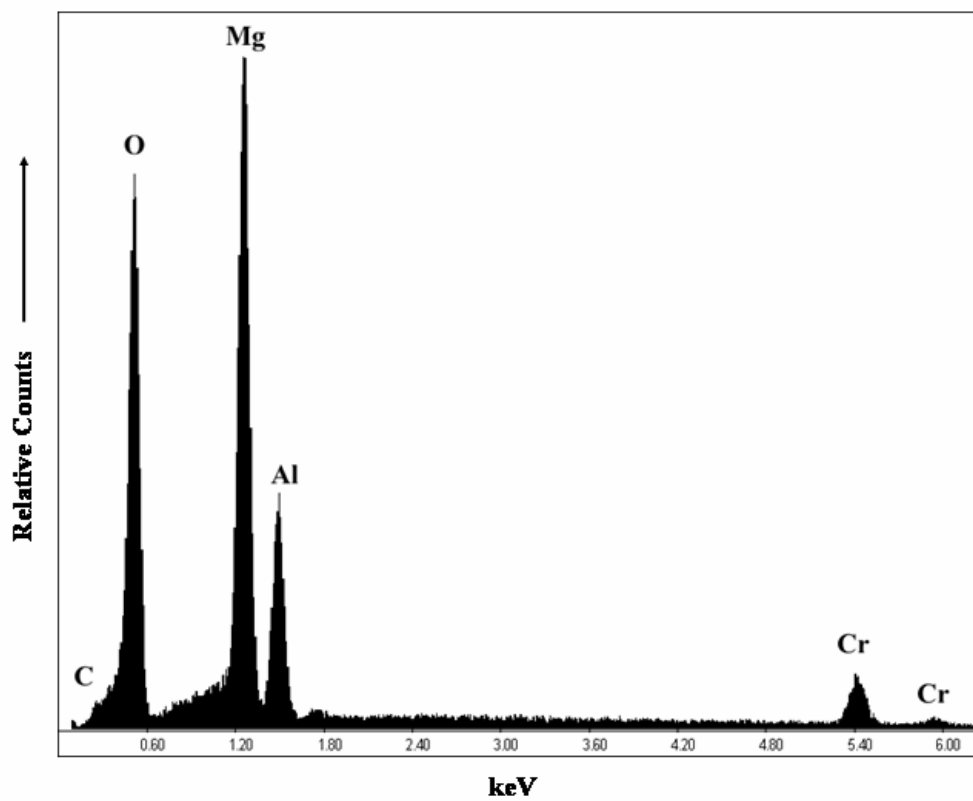


Figure 3a

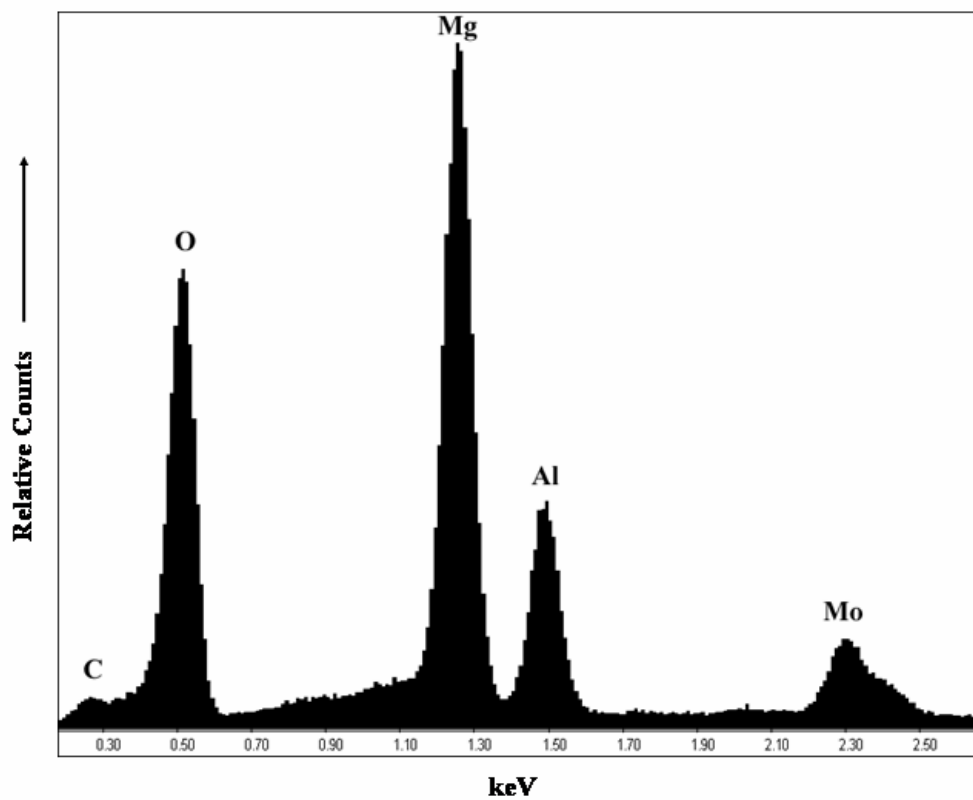


Figure 3b

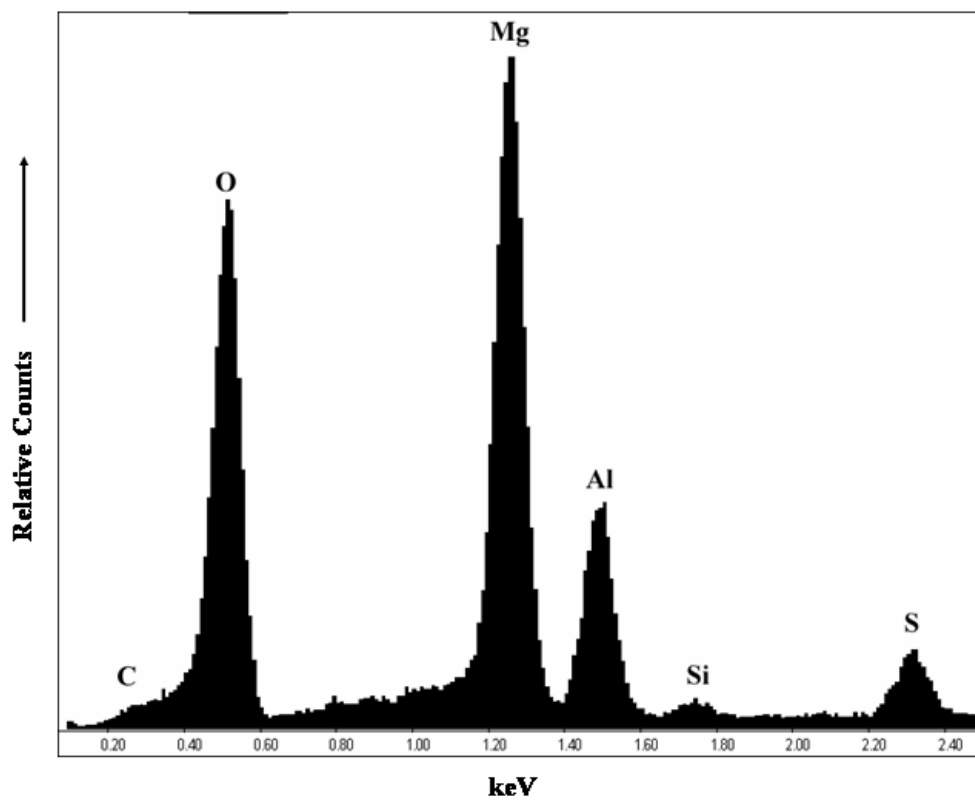


Figure 3c

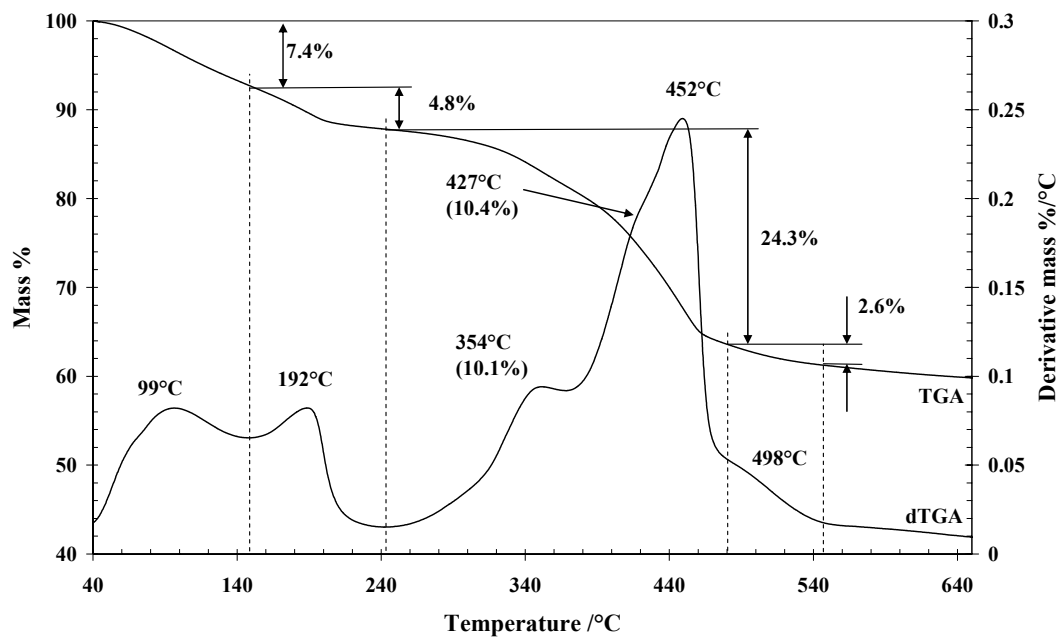


Figure 4 TG and DTG of hydrotalcite with chromate anions in the interlayer.

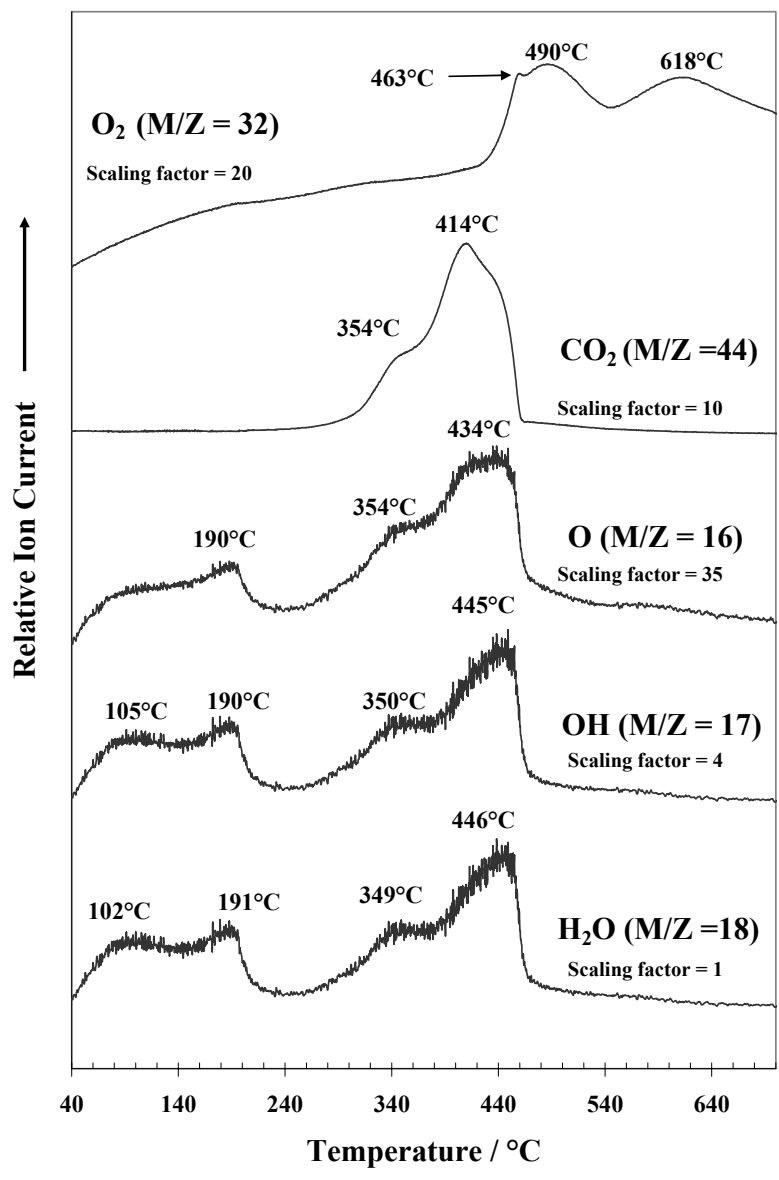


Figure 5

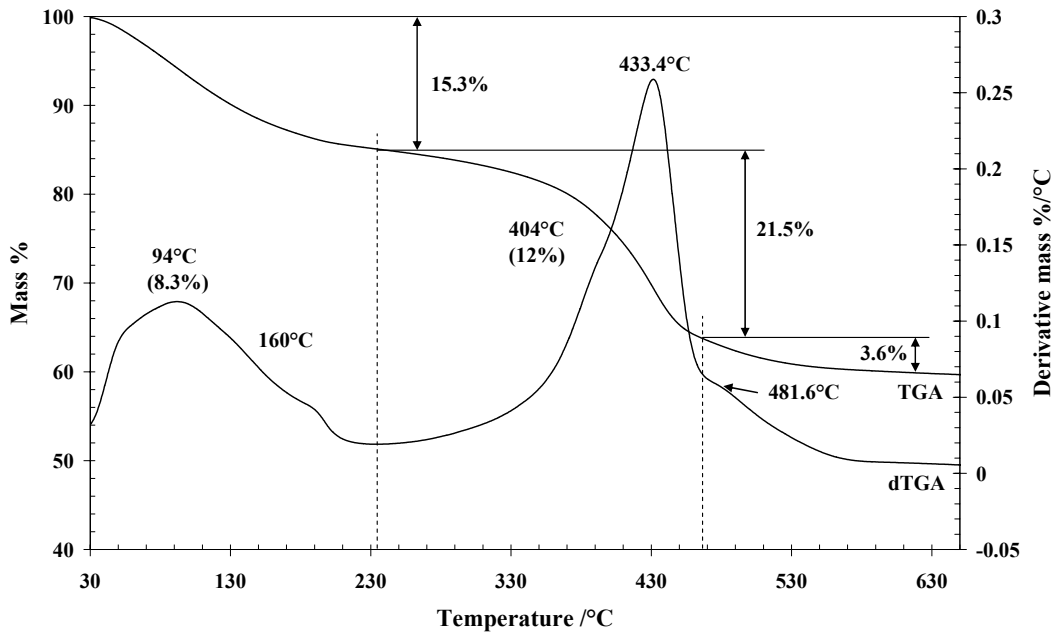


Figure 6 molybdate

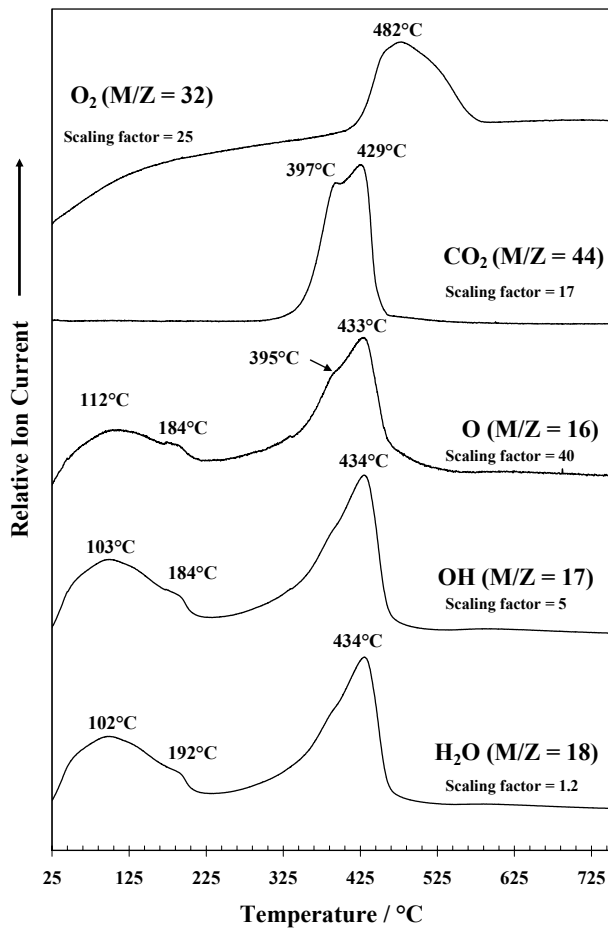


Figure 7

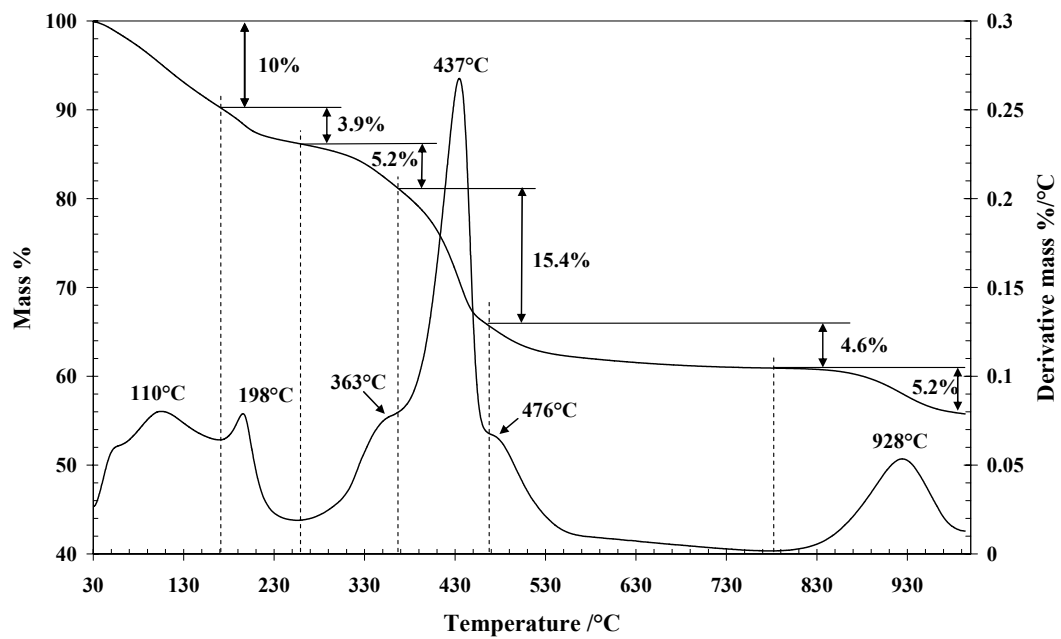


Figure 8 sulphate

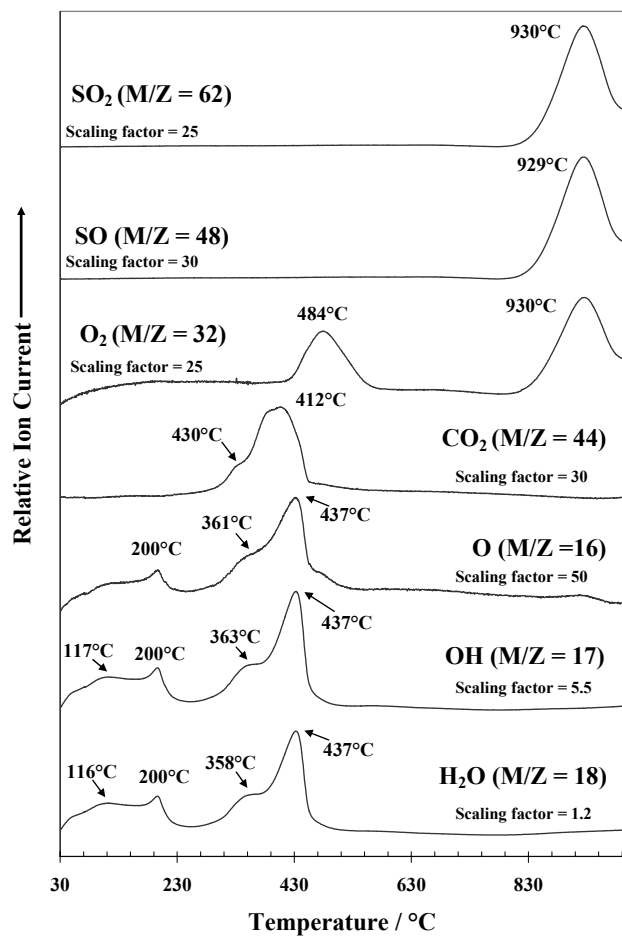


Figure 9 sulphate